

CN-Stream: Open-source library for nonlinear regular waves using stream function theory

Guillaume Ducrozet, Benjamin Bouscasse, Maïté Gouin, Pierre Ferrant, Félicien Bonnefoy*

*Ecole Centrale de Nantes, LHEEA Res. Dept. (ECN and CNRS)
1, rue de la Noë - 44321 Nantes, France*

Abstract

CN-Stream is a library for the computation of nonlinear regular ocean waves. The library is developed in order to be easily integrated with wave generation models in CFD solvers. It is based on the stream function theory and provides significant improvements regarding the applicability of the method for waves close to breaking (in deep or shallow water) compared to the classical implementation of Rienecker and Fenton [26]. The complete description of the wave field is available, including the free-surface evolution and the wave kinematics in the fluid domain. It is released as open-source, developed and distributed under the terms of GPL v3.

Keywords: Stream function, Nonlinear waves, Wave propagation, Wave kinematics, Ocean engineering.

PROGRAM SUMMARY

Manuscript Title: CN-Stream: Open-source library for nonlinear regular waves using stream function theory

Authors: G. Ducrozet, B. Bouscasse, M. Gouin, P. Ferrant, and F. Bonnefoy

Program Title: CN-Stream

Journal Reference:

Catalogue identifier:

Licensing provisions: GPL v3

Programming language: Fortran

Computer: Tested on Intel Xeon E5504 and Intel Core i7

Operating system: Any system with a Fortran compiler: tested on Linux, OS X and Windows7

RAM: Few MB for all configurations

Keywords: Stream function, Nonlinear waves, Wave propagation, Wave kinematics, Ocean engineering

Nature of problem:

CN-Stream has been developed to study the propagation of nonlinear regular waves over arbitrary constant water depth.

Solution method:

CN-Stream is an implementation of the stream function method, which solves the problem by means of finite Fourier series to reduce the free-surface conditions to a set of nonlinear equations solved by Newton's iteration method. The algorithm provides an automatic choice of the optimal number of modal components for a given accuracy.

Restrictions:

CN Stream is dedicated to the propagation of regular wave fields in infinite and finite constant depth. The evolution of irregular waves or over variable bathymetry is not treated. Furthermore, simulations are restricted to non-breaking waves.

*Corresponding author.

E-mail address: felicien.bonnefoy@ec-nantes.fr

Tel: +33 240 371 556

Fax: +33 240 372 523

Running time:

The solution is obtained in a running time of few seconds for all configurations.

Introduction

The simulation of water waves is an old topic of investigation in naval and offshore hydrodynamics. The knowledge of the incident wave field acting on a structure is important in the computation of loads. The linear description of waves is not sufficient for most realistic cases. An overview of some methods for the solution of regular waves in different conditions is presented in [28]. Regular waves are usually described either by the Stokes theory [29] or the stream function theory, for instance the one presented by Rienecker and Fenton in [26].

The important physical parameters in the context of wave propagation are the linear steepness $kH/2$ and the relative water depth kh , where $k = 2\pi/\lambda$ is the wavenumber, λ is the wavelength, H is the wave height and h is the water depth. A combination of these two parameters H/h or the Ursell number $Ur = \frac{H\lambda^2}{h^3} = 4\pi^2 \frac{kH}{(kh)^3}$ can also be used, especially in the context of reduced water depth. In ocean engineering, the limits of applicability of the different wave theories are typically taken following Le Mehauté's diagram [19] presented in Fig.1. In this figure, d stands for water depth, L for wave length, T for wave period and U_R for Ursell number.

However, it is well established that the Stokes wave theory is not accurate for very steep waves or for shallow water depths. This perturbation method is not able to provide convergent high-order Fourier coefficients [27, 7]. The solution that is usually chosen is consequently to replace the perturbation expansions by a numerical evaluation, solving a nonlinear set of equations. This is assumed to be a more suitable approach for waves close to the wave breaking limit [16]. This enhanced accuracy is particularly important for the detailed physical analysis of such phenomena but also when looking for a reference solution for waves in nonlinear potential flow formalism. For instance, it is necessary to achieve such level of accuracy when propagating waves over a long time (*e.g.* during 1000 waves periods as presented in [1, 10]) or when estimating the accuracy of a numerical model (see [12]).

The original works [3, 8, 2, 26] present different numerical solutions of the problem. The most widespread one in the ocean engineering community is probably the one described in details in [26] and simplified in [15]. In [15], the method is described and a Fortran program is provided. It uses a finite Fourier series to reduce the free surface conditions to a set of nonlinear algebraic equations, and then used Newton's iteration method to solve these nonlinear equations. This is the one taken as basis in this work.

Note that other formulations and approaches exist with the main objective of increasing the accuracy for steep waves close to the wave breaking limit in arbitrary constant water depth. We can cite *e.g.* [30] or the recent work of [32] which presents a numerical method free of any kind of approximation techniques or [6] that provides an efficient algorithm for computing steady surface gravity waves for all wavelength over depth ratios.

CN-Stream is an open-source stream function model developed at Ecole Centrale Nantes, LHEEA Res. Dept. (ECN and CNRS). The software is available to download and contribute on the GitHub platform [9]. The code is developed and redistributed under the terms of the licence GPL v3. Documentation that describes the compilation and execution of the source files is provided along with the source code. This code is one of the open-source wave models developed at Centrale Nantes. Others wave generation codes available on the GitHub platform are HOS-ocean [12], HOS-NWT [11] respectively for 2D and 3D non linear wave generation in open water and wave basin and Grid2Grid [4], which serves for their coupling with CFD (Computational Fluid Dynamics) methods.

In the following sections, the stream function theory and the corresponding numerical procedure are briefly presented together with the improvements proposed and implemented in CN-Stream. Sections describing how to compile and use the code as a library are also provided. Finally, different study cases are presented as typical applications of the presented numerical model.

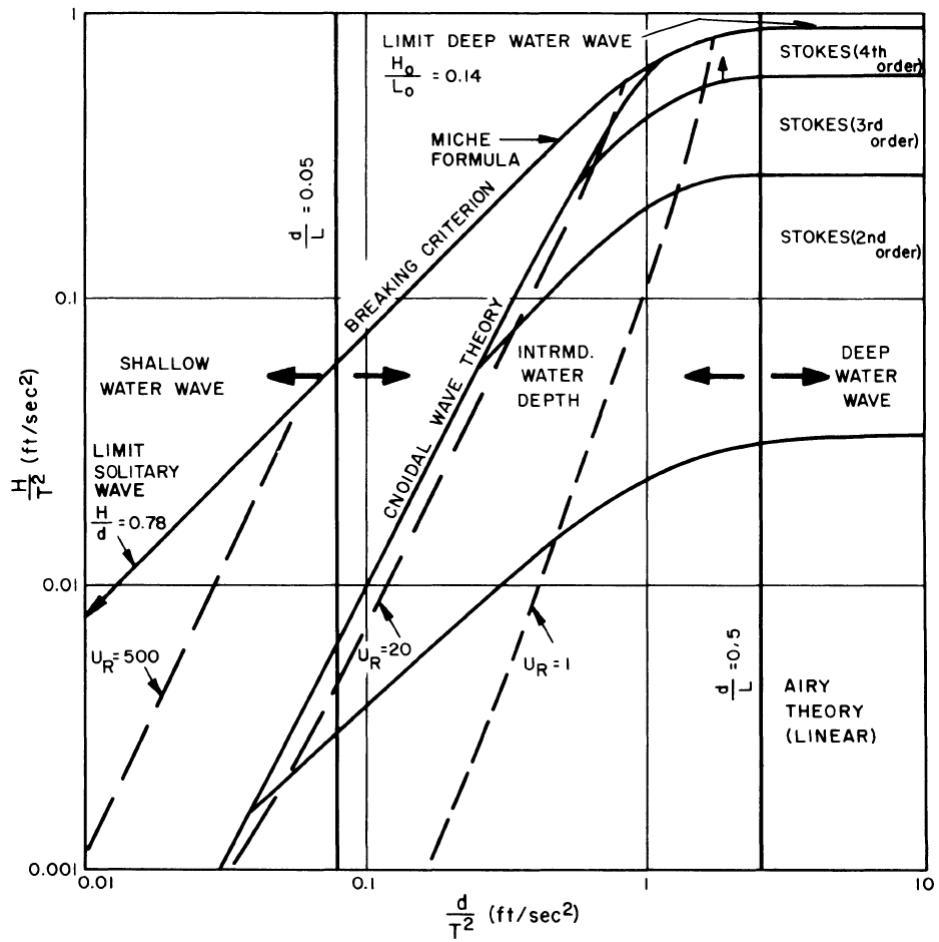


Figure 1: Le Méhauté's diagram [19]. d stands for water depth, L for wave length, T for wave period and U_R for Ursell number

One of the purposes of this code is to encourage other researchers to use this library in the context of the coupling with CFD software for wave-structure interactions modeling. Indeed, in a lot of nonlinear potential flow solvers [12, 13] or CFD softwares (SPH [23], WCCH [21], ICARE [24], OpenFOAM [18]), the incident waves are issued of the stream function theory. Some examples of the reconstructed volume fields used in CFD models are provided.

1. Stream function method

In this section, the formulation of the problem to obtain the nonlinear solution is presented in a simplified manner. More details can be found in the original work of [26] or [15], taken as basis for the numerical model CN-Stream. Some improvements of the original numerical method are then detailed.

1.1. Coordinate system

The wave propagation is solved in a fixed reference frame (O, X, Z) with the origin O taken on the free surface at rest: the horizontal axis X is oriented in the direction of the waves, and the Z axis is vertical upward.

The wave solution of the problem is assumed to be periodic both in space and time. The free surface profile is of permanent shape and the wave is propagating with a constant phase velocity c . The solution becomes stationary in a moving reference frame denoted as (x, z) . The horizontal axis x is oriented in the direction of wave propagation and the vertical axis z is upward with the origin at the free surface at rest.

$$x = X - ct \quad (1)$$

$$z = Z \quad (2)$$

Note that in the original article of [26], the origin of the vertical axis was located on the sea bed. This induces the following changes with respect to this initial work:

$$y \longrightarrow z + h \quad (3)$$

$$R \longrightarrow R + h \quad (4)$$

$$Q \longrightarrow Q + hb_0 \quad (5)$$

The exact definition of the different variables (R, Q, b_0) is presented in the following sections.

1.2. Equations

In the case of bi-dimensional isovolume flow, the stream function $\psi(x, z)$ allows for the representation of the velocity field $\mathbf{V} = (u, w) = \left(\frac{\partial\psi}{\partial z}, -\frac{\partial\psi}{\partial x}\right)$.

Furthermore, if the motion is irrotational, ψ satisfies the Laplace's equation in the fluid domain:

$$\Delta\psi = 0 \quad (6)$$

The free surface elevation is defined as $z = \eta(x)$ and the different boundary conditions are:

- the dynamic free surface boundary condition:

$$g\eta + \frac{1}{2} \left[\left(\frac{\partial\psi}{\partial x}\right)^2 + \left(\frac{\partial\psi}{\partial z}\right)^2 \right] = R, \quad \text{on } z = \eta \quad (7)$$

with R the so-called Bernoulli constant,

- a free-slip condition on the free surface $z = \eta(x)$ (also known as kinematic free surface boundary condition)
- and a free-slip condition on the bottom $z = -h$.

The free-slip boundary conditions are easily written with the stream function, which has the following properties:

- iso-lines represent the streamlines,
- the variation of the stream function between two streamlines is equal to the flow rate between those lines.

The bottom of the domain and the free surface being streamlines when considering the moving reference frame at phase velocity (and consequently permanent elevation), it is chosen to impose at the bottom:

$$\psi(x, z = -h) = 0. \quad (8)$$

As a consequence, the stream function at the free surface is related to the flow rate Q between the bottom and the free surface. This gives:

$$\psi(x, z = \eta(x)) = -Q. \quad (9)$$

In addition, the free surface presents a zero mean elevation with respect to the definition of the origin of the vertical axis. This is written as:

$$\int_0^\lambda \eta(x) dx = 0. \quad (10)$$

Then, η and ψ can be decomposed with the help of Fourier series in the horizontal plane:

$$\eta(x) = \frac{a_0}{2} + \sum_{n=1}^{+\infty} a_n \cos(k_n x) \quad (11)$$

$$\psi(x, z) = b_0 z + \sum_{n=1}^{+\infty} b_n \frac{\sinh(k_n(z+h))}{\cosh(k_n h)} \cos(k_n x) \quad (12)$$

with a_n and b_n the modal amplitudes of the free surface elevation and the stream function respectively. In the moving reference frame (x, z) , those are constant for a given wave. This equation satisfies both Eq.(6) and Eq.(8).

Equivalently, we can write the horizontal velocity u and the vertical velocity w :

$$u(x, z) = b_0 + \sum_{n=1}^{+\infty} k_n b_n \frac{\cosh(k_n(z+h))}{\cosh(k_n h)} \cos(k_n x) \quad (13)$$

$$w(x, z) = \sum_{n=1}^{+\infty} k_n b_n \frac{\sinh(k_n(z+h))}{\cosh(k_n h)} \sin(k_n x) \quad (14)$$

and the pressure is defined as:

$$\frac{p(x, z)}{\rho} = R - gz - \frac{1}{2} [u^2(x, z) + w^2(x, z)] \quad (15)$$

with ρ the water density.

1.3. Numerical solution

1.3.1. Inputs

The numerical solution needs some inputs that will define the wave to be solved. Different choices are possible for its description and the corresponding inputs are:

- the wave length λ or the wave period T

- the wave height H
- the water depth h (finite or infinite)
- the value of the current U_c that may be of two kinds: i) a Eulerian transport (the reference frame moves with respect to the fixed reference frame) or ii) a fixed mass transport velocity.

The inputs can be in dimensional or non-dimensional form.

Dimensional wave parameters. In the case of dimensional inputs, the required parameters are given in Tab.1 depending on the water depth and the known wave parameter (T or λ).

Known parameter	Infinite depth	Finite depth h
Period T	(T, H, U_c)	(T, H, h, U_c)
Wave length λ	(λ, H, U_c)	(λ, H, h, U_c)

Table 1: Dimensional input parameters for CN-Stream.

Non-dimensional wave parameters. In the case of non-dimensional value, we set non-dimensional wave height, water depth and current, denoted respectively H' , h' and U'_c . They are defined as follows (Tab. 2), depending if we know/fix as input the period or the wavelength. Note that the linear theory gives the simple following relations between the two sets of non-dimensional parameters for the wave height and the water depth:

$$\begin{aligned} H' &= \frac{H}{gT^2} = \frac{k_L H}{4\pi^2} \\ h' &= \frac{h}{gT^2} = \frac{k_L h}{4\pi^2} \end{aligned} \quad (16)$$

where k_L indicates the wave number obtained from linear dispersion relation, which is consequently slightly different from the exact wave number (see Sec. 2.3). However, for an estimate, we can also set $kH \simeq 40H'$ and $kh \simeq 40h'$.

Known parameter	Infinite depth	Finite depth h
Period T	$\left(H' = \frac{H}{gT^2}, U'_c = \frac{U}{gT} \right)$	$\left(H' = \frac{H}{gT^2}, h' = \frac{h}{gT^2}, U'_c = \frac{U}{gT} \right)$
Wave length λ	$\left(H' = kH, U'_c = \frac{U}{\sqrt{g/k}} \right)$	$\left(H' = kH, h' = kh, U'_c = \frac{U}{\sqrt{g/k}} \right)$

Table 2: Non-dimensional input parameters for CN-Stream.

1.3.2. Non-dimensional wave outputs

In the case of non-dimensional input values as described in previous section, the outputs are also made non-dimensional. This is dependent on the input:

- Wavelength as input: length scale $L_s = \lambda$ and time scale $T_s = \sqrt{\lambda/g}$
- Period as input: length scale $L_s = gT^2$ and time scale $T_s = T$

All lengths are consequently non-dimensional with length scale, for instance $\eta' = \eta/L_s$; velocities with $U' = UT_s/L_s$; etc.

1.3.3. Discretization

The free surface elevation can be studied considering its $N_2 + 1$ values at the collocation points or equivalently by expressing it on $N_2 + 1$ modes of the Fourier series:

$$\eta(x) = \frac{a_0}{2} + \sum_{n=1}^{N_2} a_n \cos(k_n x) \quad (17)$$

For the stream function, its representation in Fourier series is truncated at another number of modes chosen as $N_1 + 1$:

$$\psi(x, z) = b_0 z + \sum_{n=1}^{N_1} b_n \frac{\sinh(k_n(z+h))}{\cosh(k_n h)} \cos(k_n x) \quad (18)$$

The independent choice of N_1 and N_2 is one of the main difference with the original algorithm [14]. The motivation and implications of this choice will be detailed in Sec. 2.

Collocation points x_m are defined with respect to the free surface, fixed to a number $N_2 + 1$ between the crest and the trough of the wave (a vertical symmetry exists on half a wavelength). Previous set of equations is discretized on those collocation points such as $z = \eta(x_m)$ with $x_m = m \frac{\lambda}{2N_2}$ ($m \in [0, N_2]$).

1.3.4. Unknowns

In all configurations, the unknowns are the modal amplitudes of the stream function b_n for $n = 0$ to N_1 and the free surface elevation $\eta(x_m)$ for $m = 0$ to N_2 , the constants R and Q and the phase velocity c .

In addition we have:

- The wave number k if we specify as input the wave period T ,
- The wave period T if we specify as input the wave number k ,

This corresponds to a total number of unknowns of $N_1 + N_2 + 6$.

1.3.5. Equations

These unknowns satisfy, at a given accuracy, the following discrete nonlinear equations:

- the dynamic free surface boundary condition (Eq. (7)) written at the collocation points,

$$g\eta(x_m) + \frac{1}{2} [u(x_m, \eta(x_m))^2 + w(x_m, \eta(x_m))^2] = R, \quad m \in [0, N_2] \quad (19)$$

- the kinematic free surface boundary condition (Eq. (9)) written at the collocation points,

$$\psi(x_m, \eta(x_m)) = -Q, \quad m \in [0, N_2] \quad (20)$$

- the zero-mean free surface elevation, which is written using trapezoidal rule:

$$0 = \eta(x_0) + \eta(x_{N_2}) + \sum_{m=1}^{N_2-1} \eta(x_m), \quad (21)$$

- the fixed wave height

$$H = \max(\eta) - \min(\eta) = \eta(x_0) - \eta(x_{N_2}) \quad (22)$$

The stream function is built so that b_0 is the mean velocity of the fluid in the reference frame linked to the wave, moving at the phase velocity c . The method allows to take into account the influence of a current of two kinds:

- Eulerian transport (the reference frame is moving at a velocity c_E with respect to the fixed reference frame). This leads to the following equation: $c_E = c + b_0$,
- mass transport: $c_S = c - Q/h$.

One last equations is needed to close the system, which uses the relationship between k , c , and T :

$$k c T = 2\pi, \quad (23)$$

We consequently end up with $2N_2 + 6$ equations.

1.3.6. Numerical scheme

We assume for the numerical solution of the problem that $N_2 \geq N_1$. The system is consequently over-defined with $2N_2 + 6$ equations and $N_1 + N_2 + 6$ unknowns. Initial values for Q and R have to be given to solve the problem.

In [26], the particular case $N_1 = N_2$ is solved iteratively with a Newton-Raphson method, while least square method is used in the present implementation. The different equations to solve are expressed under the form $f(\eta(x_m), b_n, c, R, Q, T \text{ or } k) = 0$. The system is linearized at each iteration i to obtain an equation of the form:

$$A (Z^{i+1} - Z^i) = F^i \quad (24)$$

where A is the Jacobian matrix formed with the derivative of the equations with respect to the different variables, Z^i the solution vector and F^i an error vector.

If absolute errors are retained, the convergence of the solution is determined with thresholds set on $\epsilon_Z^{abs} = Z^{i+1} - Z^i$ and $\epsilon_F^{abs} = F^i - F^{i-1}$. If the convergence is controlled with relative errors, those are defined as $\epsilon_Z^{rel} = \frac{Z^{i+1} - Z^i}{\text{Scale}(Z^i)}$ and $\epsilon_F^{rel} = \frac{F^i - F^{i-1}}{\text{Scale}(F^{i-1})}$, where the function ‘‘Scale’’ ensure that the first modes are the one giving the magnitude of the solution.

1.3.7. Initial solution

The first order Stokes solution was used in [26] as the initial solution. Here we choose to impose the second-order Stokes solution, which gives the free surface elevation as:

$$\eta(x) = \frac{H}{2} \cos kx + k \left(\frac{H}{2} \right)^2 \frac{3 - \sigma^2}{4\sigma^3} \cos 2kx, \quad (25)$$

with $\sigma = \tanh kh$. The stream function at the free surface is defined as:

$$\psi(x, z = \eta) = -c + \frac{gH}{2kc} \sin kx + 3k \left(\frac{H}{2} \right)^2 \frac{1 - \sigma^2}{4\sigma^3} \sin 2kx. \quad (26)$$

Q is set to $Q = 0$ and R to $R = -c^2/2$.

1.4. From stream function to velocity potential

From the definition of the velocity potential and the stream function, we have the following equalities:

$$\frac{\partial \phi}{\partial x} = \frac{\partial \psi}{\partial z}, \quad (27)$$

and

$$\frac{\partial \phi}{\partial z} = -\frac{\partial \psi}{\partial x}. \quad (28)$$

The velocity potential ϕ is thus defined in the moving reference frame (x, z) as:

$$\phi(x, z) = b_0 x + \sum_{n=1}^{N_1} b_n \frac{\cosh(k_n(z+h))}{\cosh(k_n h)} \sin(k_n x). \quad (29)$$

When going back to the fixed reference frame (O, X, Z) , the problem becomes non-stationary. We remind that capital letters refer to the fixed reference frame, while small letters refer to the moving one, with the following change of coordinates:

$$x = X - ct \quad (30)$$

$$z = Z \quad (31)$$

$$b_0 = c + B_0 \quad (32)$$

In the fixed grid the elevation η and the velocity potential ϕ are thus defined as:

$$\eta(X, Z, t) = \frac{a_0}{2} + \sum_{n=1}^{N_2} a_n \cos(k_n(X - ct)) \quad (33)$$

$$\phi(X, Z, t) = (c + B_0)(X - ct) + \sum_{n=1}^{N_1} b_n \frac{\cosh(k_n(Z+h))}{\cosh(k_n h)} \sin(k_n(X - ct)) \quad (34)$$

And the slope used in section 2.3.2 is simply defined as:

$$\frac{\partial \eta}{\partial X}(X, Z, t) = - \sum_{n=1}^{N_2} a_n k_n \sin(k_n(X - ct)) \quad (35)$$

The horizontal velocity U and vertical velocity W are thus written as:

$$U(X, Z, t) = c + B_0 + \sum_{n=1}^{N_1} k_n b_n \frac{\cosh(k_n(Z+h))}{\cosh(k_n h)} \cos(k_n(X - ct)) \quad (36)$$

$$= c + u(X - ct, Z) \quad (37)$$

$$W(X, Z, t) = \sum_{n=1}^{N_1} k_n b_n \frac{\sinh(k_n(Z+h))}{\cosh(k_n h)} \sin(k_n(X - ct)) \quad (38)$$

$$= w(X - ct, Z) \quad (39)$$

and the pressure P :

$$\frac{P(X, Z, t)}{\rho} = R - gZ - \frac{1}{2} [u^2(X - ct, Z) + w^2(X - ct, Z)] \quad (40)$$

$$= R - gZ - \frac{1}{2} [(U(X, Z, t) - c)^2 + W^2(X, Z, t)] \quad (41)$$

Using:

$$\frac{\partial \phi}{\partial t}(X, Z, t) = -c \frac{\partial \phi}{\partial X}(X, Z, t) = -cU(X, Z, t) \quad (42)$$

it comes:

$$\frac{P(X, Z, t)}{\rho} = R - gZ - \frac{1}{2}c^2 - \frac{\partial \phi}{\partial t}(X, Z, t) - \frac{1}{2} [U^2(X, Z, t) + W^2(X, Z, t)] \quad (43)$$

1.4.1. Remarks

For some applications (see *e.g.* [12]), the dynamic free surface boundary condition Eq.(7) is written in terms of the velocity potential $\tilde{\phi}(X, Z, t)$ under the following form:

$$\frac{\partial \tilde{\phi}}{\partial t} - g\eta - \frac{1}{2} \left[\left(\frac{\partial \tilde{\phi}}{\partial X} \right)^2 + \left(\frac{\partial \tilde{\phi}}{\partial Z} \right)^2 \right] = 0, \quad \text{on } Z = \eta \quad (44)$$

This equation differs from Eq.(7) in terms of the gauge condition imposed to uniquely define the velocity potential, see [5]. The velocity potential $\phi(X, Z, t)$ does not satisfy the new dynamic boundary condition Eq.(44), leading to the definition of another velocity potential, namely $\tilde{\phi}$. The latter has to satisfy the following equation

$$\frac{\partial \tilde{\phi}}{\partial t}(X, Z, t) = \frac{\partial \phi}{\partial t}(X, Z, t) - R + \frac{1}{2}c^2, \quad (45)$$

leading to:

$$\tilde{\phi}(X, Z, t) = \left(-R + \frac{1}{2}c^2 \right) t + (c + B_0)X + \sum_{n=1}^{N_1} b_n \frac{\cosh(k_n(Z + h))}{\cosh(k_n h)} \sin(k_n(X - ct)) \quad (46)$$

Note that to keep the spatial periodicity of the potential in the x -direction, the following condition needs to be satisfied:

$$c + B_0 = 0. \quad (47)$$

This condition is satisfied if the Eulerian velocity c_E is taken equal to zero.

1.5. Improvements

1.5.1. Increments in wave height

When considering waves very close to the wave breaking limit, it appears that the numerical procedure may have some difficulty to converge toward a proper solution. In order to overcome this issue, the solution is looked for as an iterative process on the target wave height H .

The idea is to increase gradually the height of the non-linear wave, toward the final target one. At the end of one iteration, the non-linear solution for a given wave height is taken as the initial solution for the next iteration (*i.e.* a higher wave height). This allows to find an accurate solution for non-linear waves very close to the wave breaking limit, as detailed in Sec. 2.2.

The necessity of such procedure is actually related to the fact that: i) the choice of the number of modes N_1 and N_2 should be adequate to the simulated wave and ii) the second order solution is not accurate enough for highly non-linear wave. The solution procedure needs an initial guess close enough to the fully non-linear solution to be convergent.

Then, the user can specify as input the number of steps in the wave height (variable n_H of the input file), together with an increment type for these wave heights, which is either linear or exponential. As a summary, the different successive wave heights are defined as follows with H_t the target wave height, $n_H + 1$ the number of steps and $i_H \in [1, n_H + 1]$ the index of the iteration:

- Linear increment:

$$H(i_H) = \frac{i_H}{n_H + 1} H_t \quad (48)$$

- Exponential increment:

$$H(i_H) = 0.01H_t + 0.99H_t \log \left(1 + \frac{i_H - 1}{n_H} [e^1 - 1] \right) \quad (49)$$

1.5.2. Automatic evaluation of N_1 and N_2

When solving the problem, an automatic evaluation of the optimal number of collocation points (or equivalently of the number of modes) is performed. Together with the independent choice of the number of modes for the description of the stream function (or eq. velocity potential) N_1 and free-surface elevation N_2 , these represent the main enhancements of the present numerical solution compared to the original one of [26].

This routine is called after the solution of the linear system (achieved with a least square method) which uses specific numbers of modes N_1 and N_2 (see Sec. 1.3.6). Then, the number of modes is adjusted with the procedure described hereafter, leading to a new linear system (solved as in the previous step) until the convergence criteria on the choice of the number of modes is reached.

The algorithm consists in adapting the value of the number of modes for the description of the stream function (or eq. velocity potential) N_1 automatically so that the amplitude of the last mode is smaller than the target accuracy provided by the user, denoted ϵ_{N_1} .

The procedure is depicted in Fig. 2 and follows the main steps:

- Solve the problem with an initial set of values for N_1 and N_2
- Look at the modal amplitudes a_n deducing the efficient number of modes $N_{1_{eff}}$ satisfying $abs(a_{N_{1_{eff}}}) < \epsilon_{N_1}$. Then, three configurations possible:
 - if $N_{1_{eff}} < 0.4N_1$, then N_1 is decreased by 5,
 - else if $N_{1_{eff}} < N_1$ then nothing is done,
 - else N_1 is increased by 5.
- If N_1 changed, the number of modes N_2 of the elevation is deduced from N_1 by an empirical formula calibrated in section 2.3.3:

$$N_2 = N_1 \left(1.5 + \frac{1.5}{0.3} \max \left| \frac{\partial \eta}{\partial x} \right| \right). \quad (50)$$

The procedure is stopped when the solution of the problem is achieved at the target accuracy (iterative solution of the linear system) and when the number of modes is unchanged in the previous algorithm, meaning it is optimal for the current configuration.

2. Results

This section presents different results obtained with the CN-Stream code. The objective of this part is to detail the numerical properties of the method and especially to demonstrate the relevance of the enhancements proposed. The highest waves accessible with the current method are also provided explicitly as a matter of completeness.

In addition, different applications of the CN-Stream model to the study of non-linear regular waves are presented. In the text some references are done to the parameters names in the input files, which are further described in section 3.3.1.

2.1. Some examples: Modal description of quantities

In this paragraph three different wave conditions are simulated corresponding respectively to infinite, finite and shallow water depths. The corresponding wave parameters are given in Tab.3. For each wave condition, the elevation and the slope are presented as a function of the phase kx , as well as the modal amplitudes of the elevation and velocity potential. Then, the maximal steepnesses available for different water depths are presented.

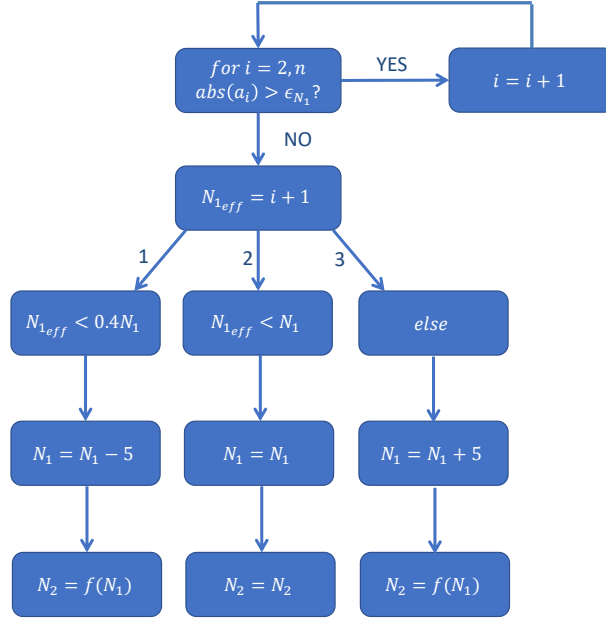


Figure 2: Automatic calculation of N_1 and N_2 performed in CN-Stream.

	Period (s)	Height (m)	Depth (m)	H/gT^2	kH	h/gT^2	kh
Infinite water depth	8	15	Inf	0.024	0.80	Inf	Inf
Finite water depth	8	14	37	0.022	0.78	0.059	2.0
Shallow water depth	25	10	37	0.0016	0.13	0.006	0.48

Table 3: Wave parameters for the three studied conditions.

2.1.1. Infinite water depth

In Fig.3, an example of a wave propagating over an infinite water depth with a wave period $T = 8\text{s}$ and a wave height $H = 15\text{m}$ is presented. The wave surface elevation and the slope are shown as well as the modal amplitudes of the free surface elevation η and the velocity potential ϕ .

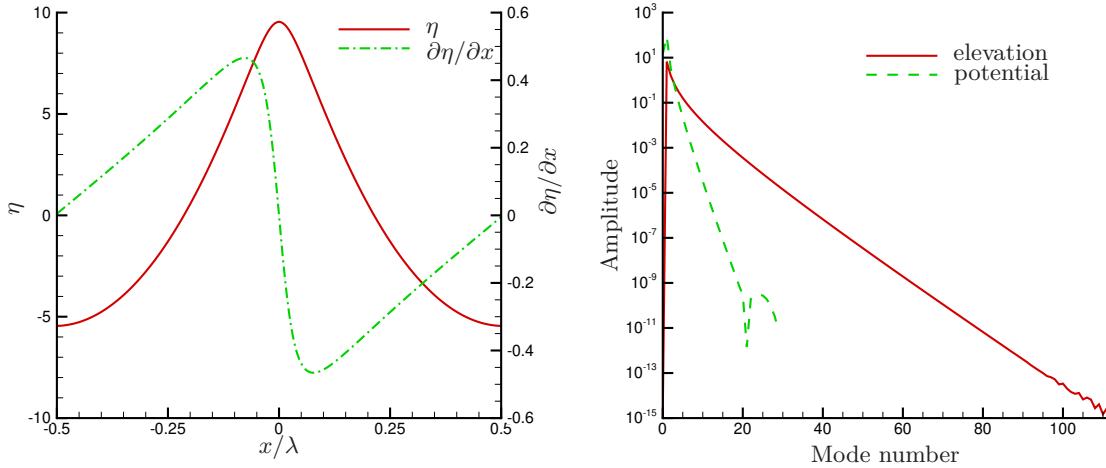


Figure 3: Infinite water depth - wave period $T = 8\text{s}$ and wave height $H = 15\text{m}$. Left: Wave surface elevation and slope. Right: Modal amplitudes of the surface elevation and of the velocity potential.

For such high steepness $kH = 0.80$, the well-known non-linear features of the free surface elevation are recovered, namely a strong asymmetry between the crest and the trough, together with large value of the local steepness.

It is also clear from the modal description that the necessary number of modes is different for η and ϕ due to a different convergence rate of the modal amplitudes. Thanks to the proposed enhanced algorithm, one can reach an accuracy on the amplitude of the mode of $\epsilon_{N_1} = 10^{-12}$ (defined as relative error).

As a matter of comparison to the original stream function model [26], the same algorithm is applied, fixing the same number of modes for the two quantities (*i.e.* $N_1 = N_2$). The results are depicted in Fig. 4.

The free surface looks the same than previously in the spatial domain, but even if the modal description of η and ϕ are still convergent, the level of accuracy is reduced compared to the enhanced stream function model. The results of Fig. 4 are actually the highest accuracy (*i.e.* smallest amplitude of highest mode) one can possibly reach when using $N_1 = N_2$. The amplitude of the smallest mode for the description of the free surface elevation is now $\epsilon = 2 \cdot 10^{-5}$ to compare with $\epsilon_{N_1} = 10^{-12}$ in the previous configuration.

The accuracy is actually limited by the fact that if one increases the number of modes for the description of η , the consequent increase in the description of ϕ may create some numerical instabilities. As an example, Fig. 5 depicts the initiation of such process for a regular wave in infinite depth with a smaller wave height ($T = 8\text{s}$ and wave height $H = 11\text{m}$).

For this wave steepness, one can reach a relative amplitude of the smallest mode $\epsilon = 5 \cdot 10^{-11}$. It is clearly seen that the decrease of the modal amplitudes of the velocity potential reach a plateau after the mode number 16 – 17. These highest modes, which do not decrease in amplitude any more are responsible of the enhanced behaviour observed of CN-Stream compared to original implementation of [26]. This comes from the involved spatial derivatives of the quantities, corresponding to a multiplication by k in the modal space that will induce a non convergent Fourier description of the corresponding quantity.

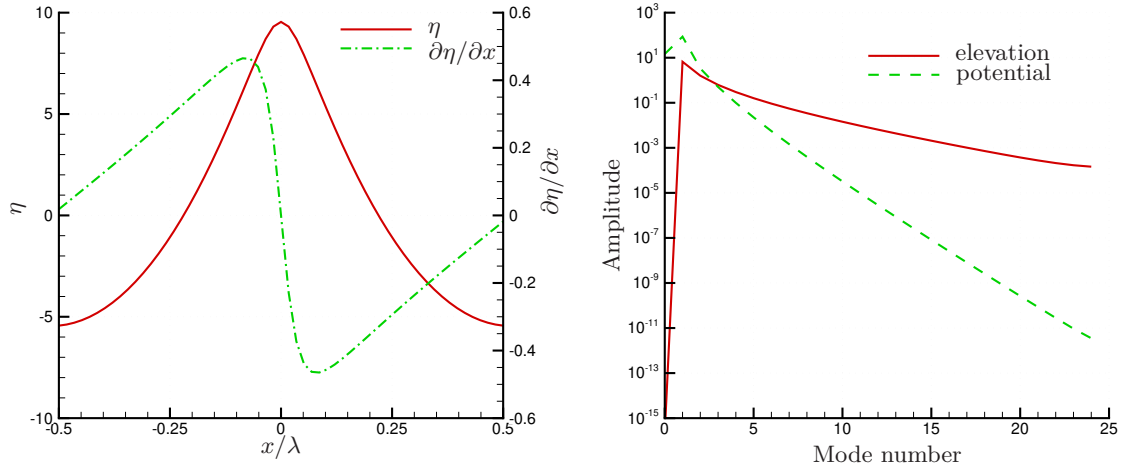


Figure 4: Infinite water depth - wave period $T = 8$ s and wave height $H = 15$ m. Non-optimal CN-Stream solution with $N_1 = N_2$. Left: Wave surface elevation and slope. Right: Modal amplitudes of the surface elevation and of the velocity potential.

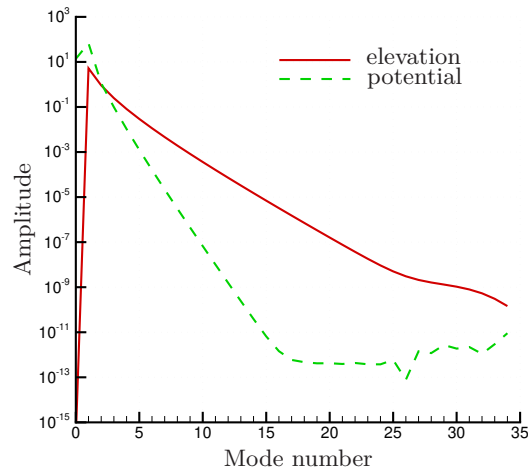


Figure 5: Infinite water depth - wave period $T = 8$ s and wave height $H = 11$ m. Non-optimal CN-Stream solution with $N_1 = N_2$. Modal amplitudes of the surface elevation and of the velocity potential.

2.1.2. Finite water depth ($h' = h/gT^2 = 0.059$ and $kh = 2.0$)

In Fig.6, an example of a non-linear regular wave propagating over a finite water depth ($h = 37\text{m}$) with a wave period $T = 8\text{s}$ and a wave height $H = 14\text{m}$ is presented. The wave surface elevation and the slope are shown as well as the modal amplitudes of η and ϕ .

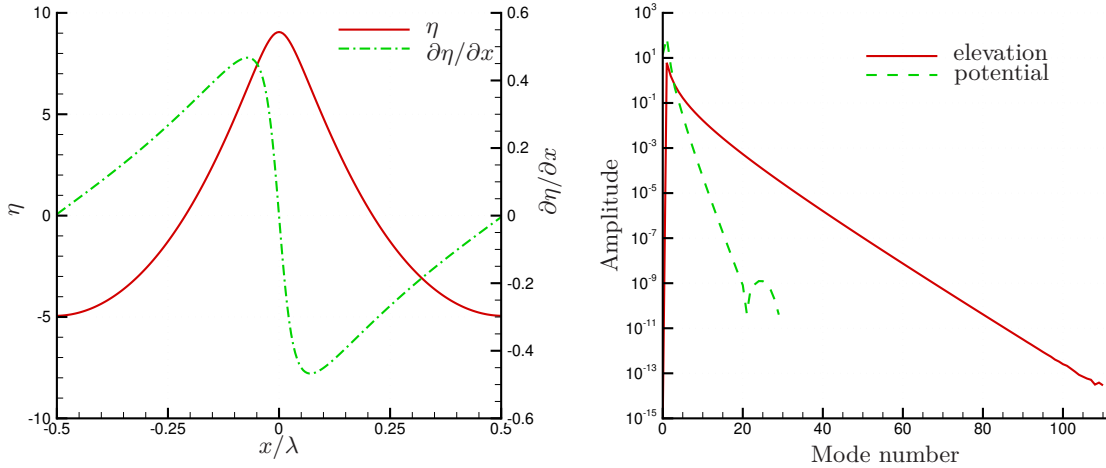


Figure 6: Finite water depth - wave period $T = 8\text{s}$, wave height $H = 14\text{m}$ and water depth $h = 37\text{m}$. Left: Wave surface elevation and slope. Right: Modal amplitudes of the surface elevation and of the velocity potential.

This configuration is usually known as intermediate water depth ($kh = 2.0$) with consequently limited effect of the presence of the sea floor. Comparing with Fig. 3, the results are similar with a free surface profile exhibiting slightly longer troughs and a modal description requiring similar number of modes ($N_1 = 30$ and $N_2 = 111$) to reach the same accuracy $\epsilon_{N_1} = 10^{-12}$.

2.1.3. Shallow water depth ($h' = h/gT^2 = 0.006$ and $kh = 0.48$)

The last example in this part deals with a wave propagating over a the same water depth than previous one ($h = 37\text{m}$) but with a significantly longer wave period $T = 25\text{s}$. This corresponds to a shallow water wave configuration ($kh = 0.48$) and a wave height $H = 10\text{m}$. The wave surface elevation and the slope are shown as well as the modal amplitudes of η and ϕ in Fig.7.

The physical effects associated to the shallowness of the water depth are now clear in this configuration with very clear assymetries between crest and trough in the horizontal and the vertical directions. In terms of modal representation, it is interesting to note that when going to shallower water depth, the decrease rate of the modal amplitudes of η and ϕ becomes closer one with the other. As a consequence, the necessary number of points to reach the target accuracy $\epsilon_{N_1} = 10^{-12}$ is now $N_1 = 25$ and $N_2 = 49$.

2.2. Limiting waves

It appears interesting for the user to have an idea of the waves that can be computed with CN-Stream. We remind that the important physical parameters are the steepness kH and the relative water depth kh (or a combination of these two parameters such as height to depth ratio H/h or the Ursell number $Ur = \frac{H\lambda^2}{h^3} = 4\pi^2 \frac{kH}{(kh)^3}$).

The results are dependent of the numerical parameters. The following parameters are used in the present section (in brackets the corresponding input file option, see section 3 for details):

- $n_H = 100$ (option: `n_H`)

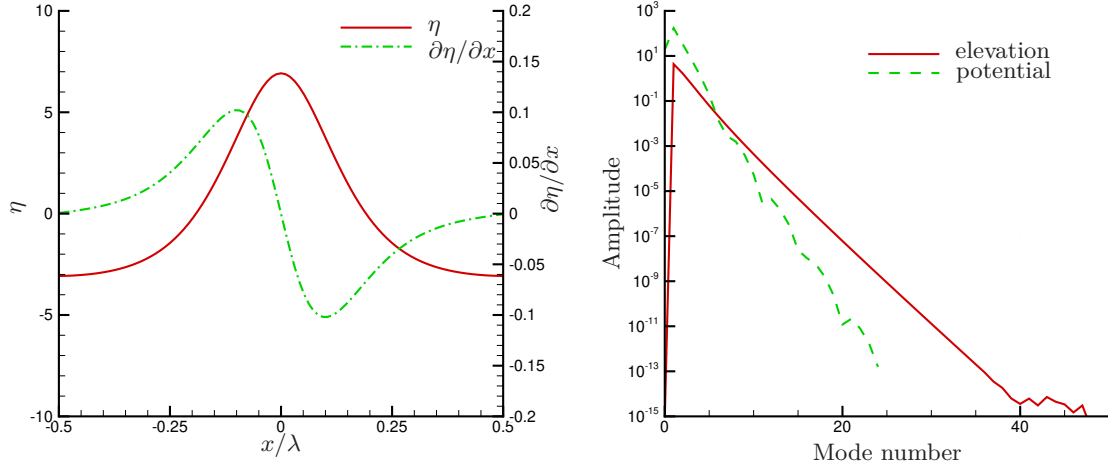


Figure 7: Finite water depth - wave period $T = 25$ s, wave height $H = 10$ m and water depth $h = 37$ m. Left: Wave surface elevation and slope. Right: Modal amplitudes of the surface elevation and of the velocity potential.

- Relative error (option: `err_type = 1`)
- $\epsilon_F^{rel} = 10^{-10}$ (option: `eps_err`)
- $\max(\epsilon_F^{rel}) = 10.0$ (option: `err_max`)
- $\epsilon_Z^{rel} = 10^{-10}$ (option: `eps_inc`)
- $\epsilon_{N_1} = 10^{-10}$

Moreover, computations are performed in non-dimensional form (waveInput: GeneralDimension = 0 see section 3) and without any eulerian current (input: CurrentType=0 and input: CurrentValue=0.0). Tables 4 & 5 present the numerical values obtained for the different tests that have been performed. H_{lim} stands for the highest wave accessible with CN-Stream in the configuration tested.

Input is λ (input: WaveInput=1)							
Relative water depth kh	∞	3.0	1.0	0.5	0.3	0.2	0.1
Limiting steepness kH_{lim}	0.84	0.84	0.60	0.34	0.22	0.15	0.077
H_{lim}/h	undef.	0.28	0.60	0.68	0.72	0.74	0.77

Table 4: Maximal steepnesses that can be computed for different water depths - non-dimensional input is the wavelength λ .

Input is T (input: WaveInput=0)							
Relative water depth $h/(gT^2)$	∞	0.1	0.02	0.005	0.002	0.001	0.0005
Limiting steepness $H_{lim}/(gT^2)$	0.025	0.025	0.012	0.0035	0.0015	0.00075	0.00038
H_{lim}/h	undef.	0.25	0.61	0.70	0.73	0.75	0.76

Table 5: Maximal steepnesses that can be computed for different water depths - non-dimensional input is the period T .

In order to be clearer and to compare the results presented in Tabs. 4 & 5 to the theoretical formulas of limiting regular waves in various conditions, the preceding results are plotted in Figs. 8 & 9.

Limits to the existence of waves have been first parametrized by [22]. He proposed a simple formula for the maximal steepness that can be computed given by:

$$\epsilon_{lim} = H_{lim}/\lambda, \quad (51)$$

for a large range of depths h . This equation (51) has been validated thanks to experimental and numerical data and takes now the following form:

$$\epsilon_{lim} = 0.142 \tanh(kh). \quad (52)$$

It should be noted that in very shallow water depths ($kh \rightarrow 0$), this equation (52) overestimates the maximum computed height ($H_{lim}/h \rightarrow 2\pi * 0.142 = 0.892$). Various studies have tried to improve this simple formula. For instance [31] studied experimentally the gravity waves stability in a large range of relative water depths. [16] used the experimental results to propose a parametrized formula under the form:

$$\frac{H_{lim}}{h} = \frac{0.141063 \left(\frac{\lambda}{h}\right) + 0.0095721 \left(\frac{\lambda}{h}\right)^2 + 0.0077829 \left(\frac{\lambda}{h}\right)^3}{1 + 0.0788340 \left(\frac{\lambda}{h}\right) + 0.00317567 \left(\frac{\lambda}{h}\right)^2 + 0.0093407 \left(\frac{\lambda}{h}\right)^3}. \quad (53)$$

This formula presents the advantages to accurately treat the following limiting cases:

- infinite depth and $kH_{lim} = 0.885$,
- solitary wave in very shallow water depth $H_{lim}/h = 0.833$ (see for instance [17])

The two preceding equations (52) & (53) use non-dimensional quantities with respect to the wavelength λ . It can also be useful to non-dimensionalize the quantities by the period, as presented in Le Méhauté's diagram (see Fig. 1, Fig. 9 and [19]). This diagram presents the limit in terms of wave height $H_{lim}/(gT^2)$ as function of the relative water depth $h/(gT^2)$.

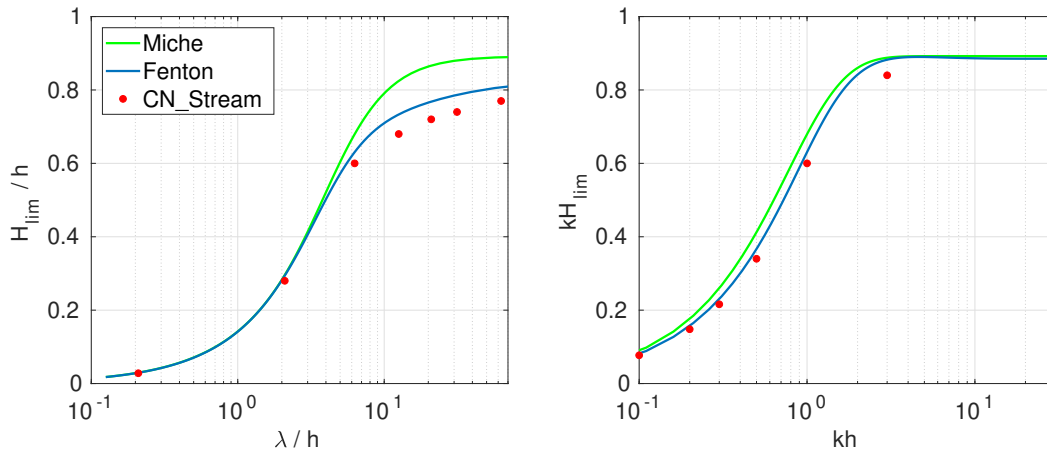


Figure 8: The region in which solutions for steady waves can be obtained with CN-Stream (dots representing the highest wave accessible H_{lim} for given input parameters). Comparison to the theoretical formulas of [22] and [16]. Input is the wavelength.

As a summary, with the chosen high level of accuracy, those results demonstrate that the CN-Stream code allows the simulation of non-linear regular waves up to waves close to the breaking limit. If one intends to simulate even higher waves, the acceptable level of error needs to be reduced.

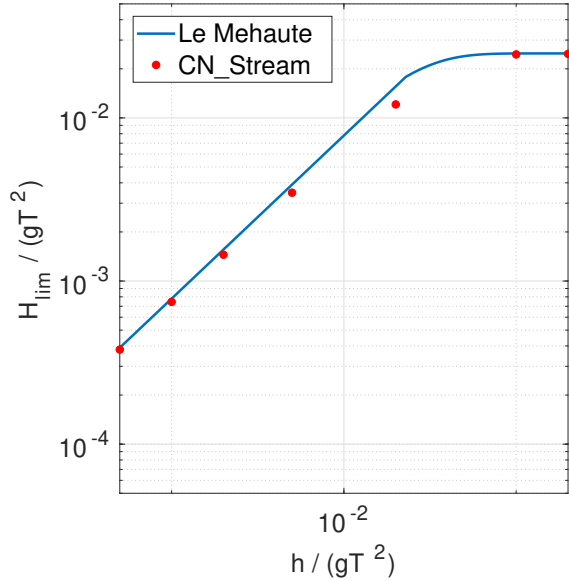


Figure 9: The region in which solutions for steady waves can be obtained with CN-Stream (dots representing the highest wave accessible H_{lim} for given input parameters). Comparison to the theoretical formulas of [19]. Input is the period.

2.3. Nonlinear effects

This section is dedicated to the study of some of the non-linear features associated to regular water waves. These are useful in the definition of some properties for the numerical solution.

2.3.1. Influence on the wavelength

Infinite water depth. In infinite water depth, the only non-dimensional parameter characterizing the wave is the steepness. Figure 10 (left) shows the evolution of the wavelength with the "real" slope (measured as the maximum of the slope $|\partial\eta/\partial x|$ over the wavelength). A good agreement is found with the third-order formula:

$$\frac{\lambda_{NL}}{\lambda_L} = 1 + (ka)^2, \quad (54)$$

with $ka = \frac{kH}{2} = \max |\partial\eta/\partial x|$, until $ka \simeq 0.3$.

The evolution of the two different definitions for the steepness ($kH/2$ and maximum slope) as a function of the non-dimensional height $H' = H/gT^2$ is also provided in Fig. 10. It appears that the steepness defined as the maximum slope as an almost linear dependence with H' over the whole range of existence of the wave (except for the most extreme ones), while $kH/2$ exhibits a more complex evolution, which is linear only for waves with moderate steepness.

All water depths. Then, Fig.11 shows the non-linear evolution of the wavelength as a function of the maximal wave slope. The whole range of depths is covered from shallow water depths to infinite water depths, as shown in Tab. 6.

$k_L h$	0.2	0.4	0.8	1.6	3.2
$h' = h/gT^2$	0.005	0.01	0.02	0.04	0.08

Table 6: Non-dimensional depths.

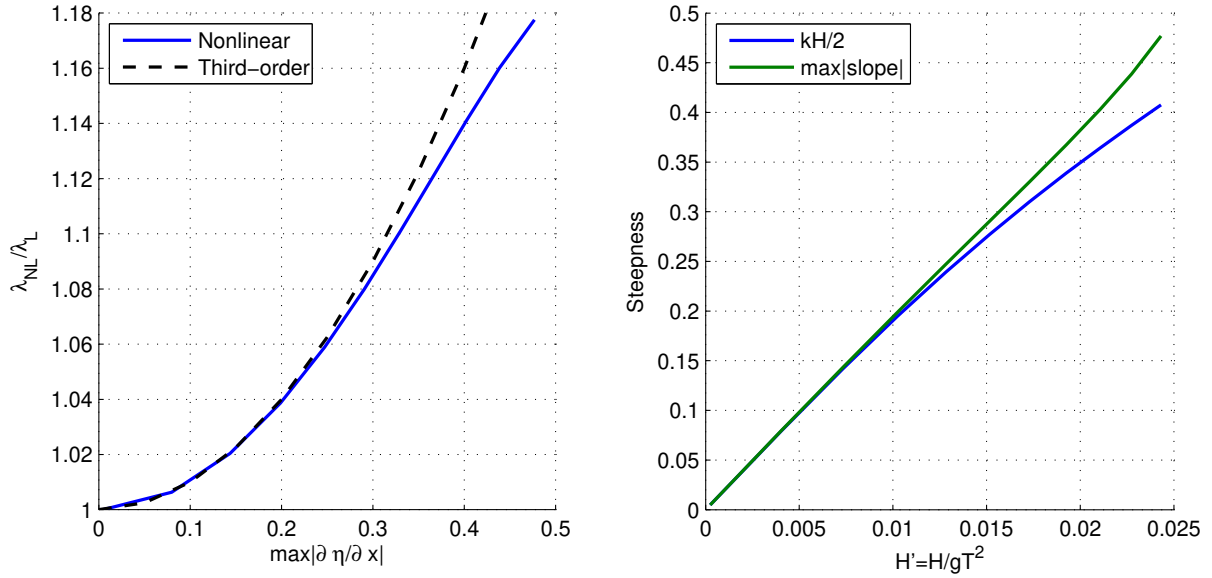


Figure 10: Wavelength (left) and steepness (right) evolutions for a wave propagating over an infinite water depth.

For small slopes, the increase of the wavelength is more important for small relative water depths. For larger slopes, the modification of the wavelength does not exhibit a specific trend with the relative water depth anymore, even if the shallower water depth seems to always exhibit the largest increase in non-linear wave length.

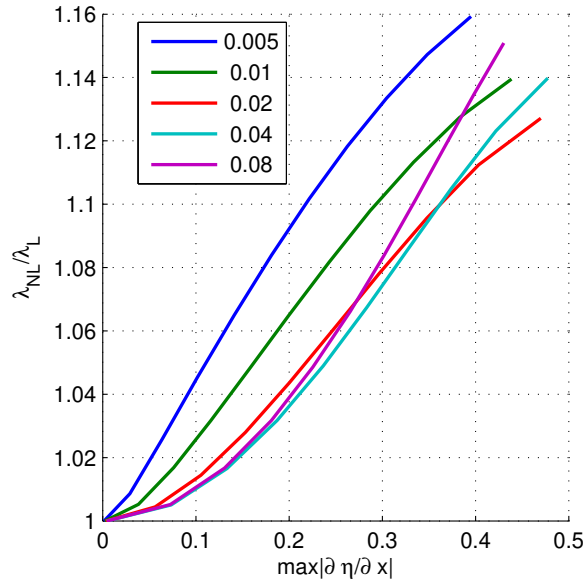


Figure 11: Non-linear evolution of the wavelength for a wave propagating in finite water depths (the legend gives the values of $h' = h/gT^2$).

Note that depending on the relative water depth, the maximum slope observed for the steepest wave com-

puted is varying in the range $\max |\partial\eta/\partial x| \in [0.40; 0.48]$. Similarly, we observe that the maximal modification in wave length is in a small range [13%; 16%].

The non-linear modification of the wavelength is consequently moderate. There is thus no explicit need to use the non-linear wavelength when computing the non-dimensional parameters such as kh and kH .

Figure 12 presents the wave elevation obtained for the maximal slope at various water depths.

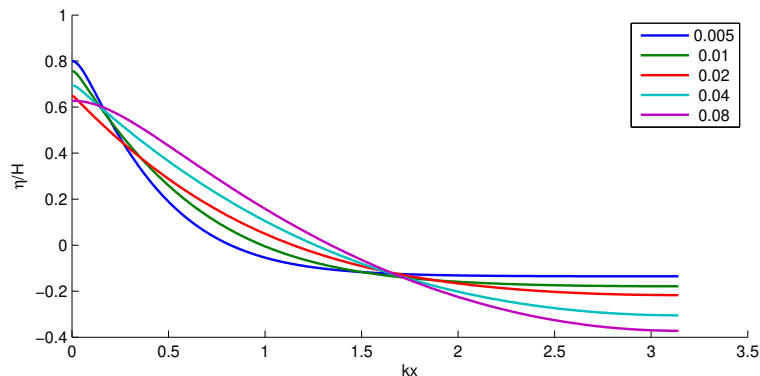


Figure 12: Wave elevation obtained for a maximal slope (the legend gives the values of $h' = h/gT^2$).

As expected, the crest-trough asymmetry is enhanced when reducing the relative water depth (both in terms of amplitude and relative length). The numerical solution of CN-Stream in small water depth recovers the cnoidal wave features.

2.3.2. Maximal slope

Infinite water depth. It is interesting to compare the various definitions of the steepness (the linear steepness $kH/2$ and the maximal slope) as a function of the relative wave height $H' = H/gT^2$. The following relationship is expected:

$$H' = \frac{H}{gT^2} = \frac{k_L H}{2} \frac{1}{2\pi^2} \quad (55)$$

with $2\pi^2 \simeq 19.7$. From Fig.10 (right) we observe that $\max |\partial\eta/\partial x| = 19H'$ for all H' . It means that H' is a very good measurement of the wave slope non-linearity for the infinite water depth case. The linear steepness $kH/2$ is moving away from the maximal wave slope as soon as $H' > 0.015$.

All water depths. The evolution between the slope and H' is presented in Fig.13 for different water depths. One can observe that the relative water depth $k_L h = 3$ ($h' = 0.08$) already corresponds to the infinite water depth: results for larger water depths are superimposed to those obtained at $k_L h = 3$. This corresponds to the usual definition of waves considered as deep-water when $h/\lambda > 0.5$.

For an infinite water depth (see paragraph above), we observed that H' was proportional to the maximal wave slope for all wave steepnesses. Here, Fig. 13 shows that for a shallow water depth, the relationship between H' and the steepness is linear only for small slopes. Thus the parameter H' is not a good measurement of the wave non-linearity in shallow water. Indeed, if the value of H' is multiplied by 2, the maximal wave slope is multiplied by a factor larger than 2, showing that the wave non-linearity increases faster than the wave height in shallow water depths.

It is also observed in Fig.13 that when varying the wave height, the value of the maximal steepness varies between 0.43 and 0.6, whatever the depth h' . The wave steepness is thus a good indicator of the non-linearities, even if the maximal slope is the most relevant one, as noticed in Fig. 11.

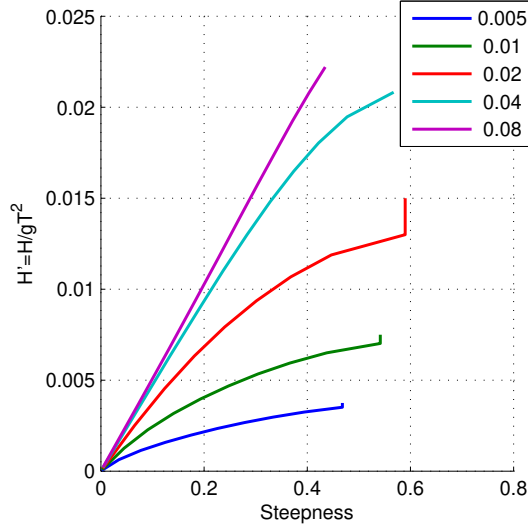


Figure 13: Steepnesses for a wave propagating over a finite water depth (the legend gives the values of h').

2.3.3. Choice of N_1 and N_2

As previously, the whole range of relative water depths was covered from shallow to deep water, as presented in Tab. 6. In this section, the following numerical parameters have been used:

- $\epsilon_F^{rel} = 10^{-12}$, (option: eps_err)
- $\max(\epsilon_F) = 10.0$ (option: err_max)
- $\epsilon_Z^{rel} = 710^{-14}$ (option: eps_inc)
- $\epsilon_{N_1} = 10^{-14}$ (option: eps_N1)

For a given wave period T , a given wave height H and a given water depth h , one can evaluate the non-dimensional numbers H' and h' . Then, thanks to Fig. 13, one can deduce the maximal slope.

In order to achieve the convergence on the amplitude of the modes (input parameter option: eps_N1), the number of modes N_1 and N_2 are plotted as a function of the slope in Fig.14. It can be observed, as expected, that when increasing the slope, an increased number of modes is necessary. This is associated to the need of a larger number of modes in shallow water depth than in infinite depth at a given slope. For instance, for the maximal slope achievable, 50 (200) modes for $\phi(\eta)$ are necessary in shallow water depth and 20 (60) in infinite depth.

As a matter of simplification of the numerical procedure, Fig. 15 shows the evolution of the ratio N_2/N_1 as a function of the slope.

We observe that this ratio N_2/N_1 is almost constant for any water depth. This allows us to extract the following relationship between those two number of modes:

$$N_2 = N_1 \left(1.5 + \frac{1.5}{0.3} \max \left| \frac{\partial \eta}{\partial x} \right| \right). \quad (56)$$

This reduces to only one parameter the procedure for an automatic choice of the number of modes, as described in 1.5.2.

2.4. Kinematics and pressure inside the domain

This final section presents some examples of velocity and pressure fields obtained with CN-Stream. This illustrates the possibilities of the numerical model to provide informations about the incident wave field in view of possible coupling with CFD software for wave-structure interactions modeling.

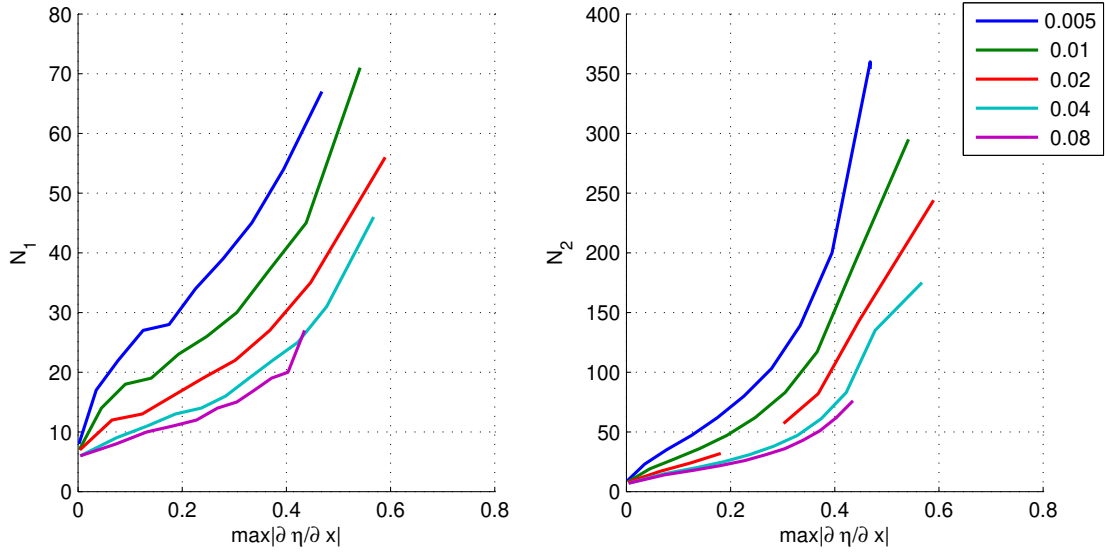


Figure 14: Necessary modes for the velocity potential (N_1 , left) and for the elevation (N_2 , right) for a wave propagating over a finite depth (the legend gives the values of $h' = h/gT^2$).

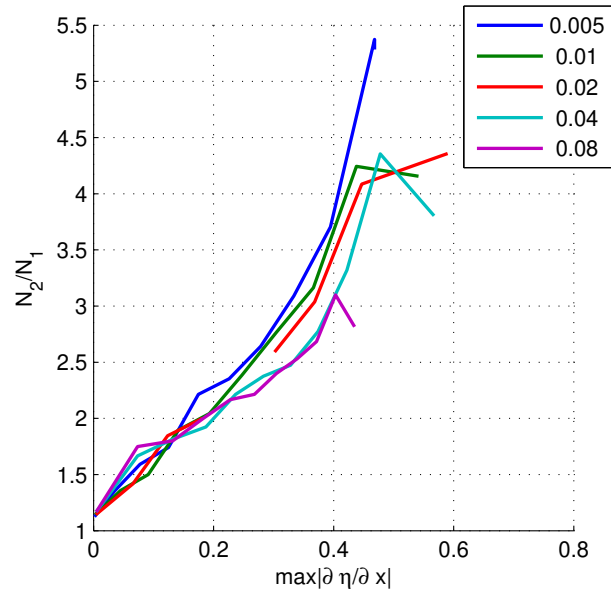


Figure 15: Ratio of N_2/N_1 for a wave propagating over a finite depth (the legend gives the values of h').

2.4.1. Finite water depth

The finite water depth case presented in Tab. 3 along with the option parameters used in Section 2.3.3 is computed and a reconstruction of the volume fields is performed, as presented in Fig. 16.

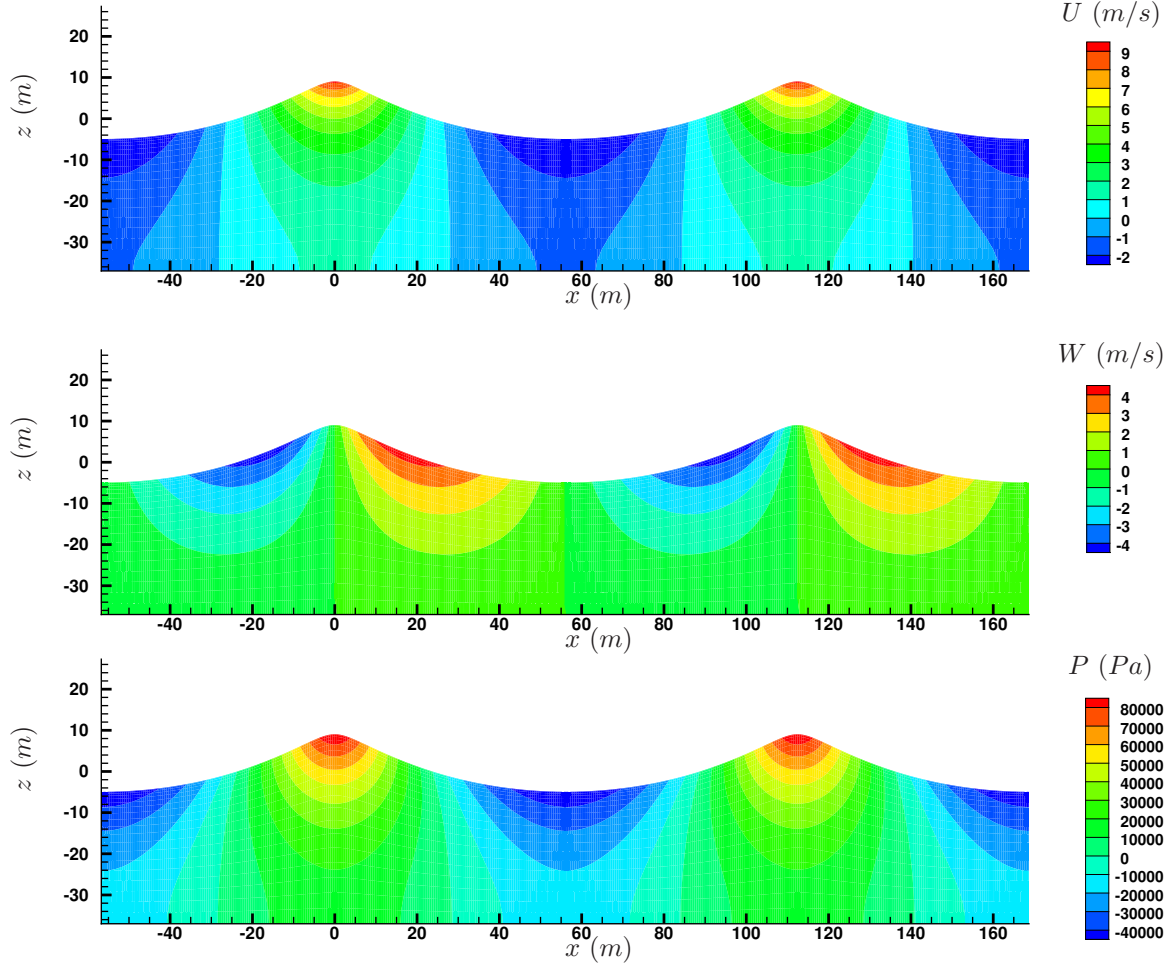


Figure 16: Horizontal velocity field (up), vertical velocity field (middle) and dynamic pressure field (bottom) for a wave propagating over a finite water depth $kh = 2$ and $kH = 0.78$.

The horizontal velocity appears highly non-linear with large differences between the values in the crests and in the troughs ($\max(U) \simeq 9 \text{ m/s}$ and $\min(U) \simeq -3 \text{ m/s}$). Similarly, the dynamic pressure field exhibits larger absolute values in the crests than in the troughs (difference is around 80 %).

2.4.2. Shallow water depth

The shallow water depth case presented in Tab.3 along with the option parameters used in Section 2.3.3 is computed and a reconstruction of the volumic fields is performed, as presented in Fig. 17.

The non-linear features observed previously at a larger relative water depth are further enhanced with the reduced water depth. The strong asymmetry in the free surface profile (both in horizontal and vertical directions) is also observed in both the velocity and the pressure field.

The necessary use of fully non-linear potential wave theories in the context of highly non-linear waves, close to the wave breaking limit, is clearly demonstrated. The wave kinematics and induced pressure fields

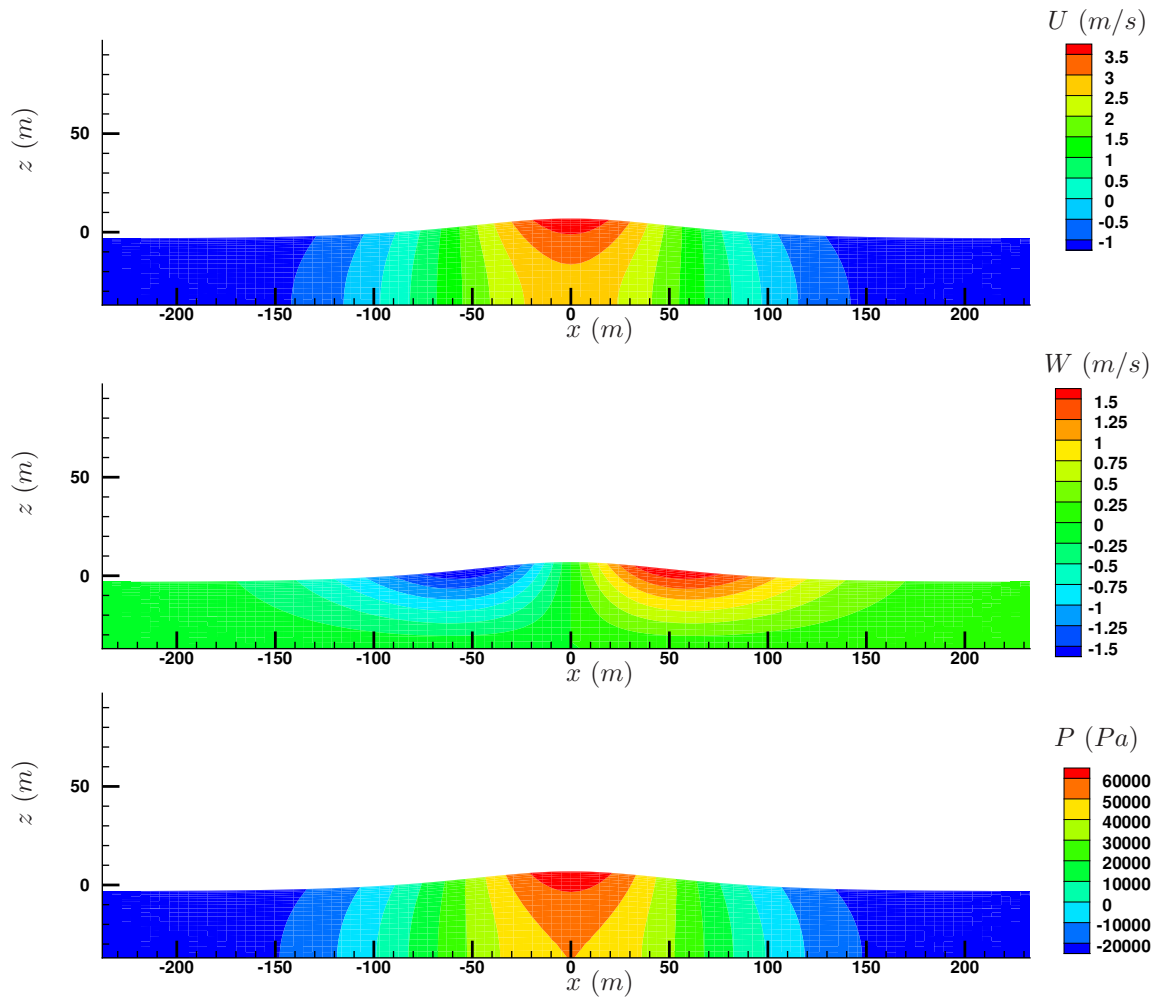


Figure 17: Horizontal velocity field (up), vertical velocity field (middle) and dynamic pressure field (bottom) for a wave propagating over a shallow water depth $kh = 0.48$ and $kH = 0.13$.

are strongly influenced by the wave non-linearity.

3. Program documentation

CN-Stream is a computational program written in Fortran language. It can be compiled as an executable file for the study of specific wave problems with inputs and dedicated outputs to be detailed in the following sections. It can also be used as a static library, which can easily be linked to other numerical models in the objective of, for instance, solve the problem of wave-structure interactions.

Figure 18 presents an overview of the algorithm at use in CN-Stream. The main subroutines of the program are detailed with their respective purposes.

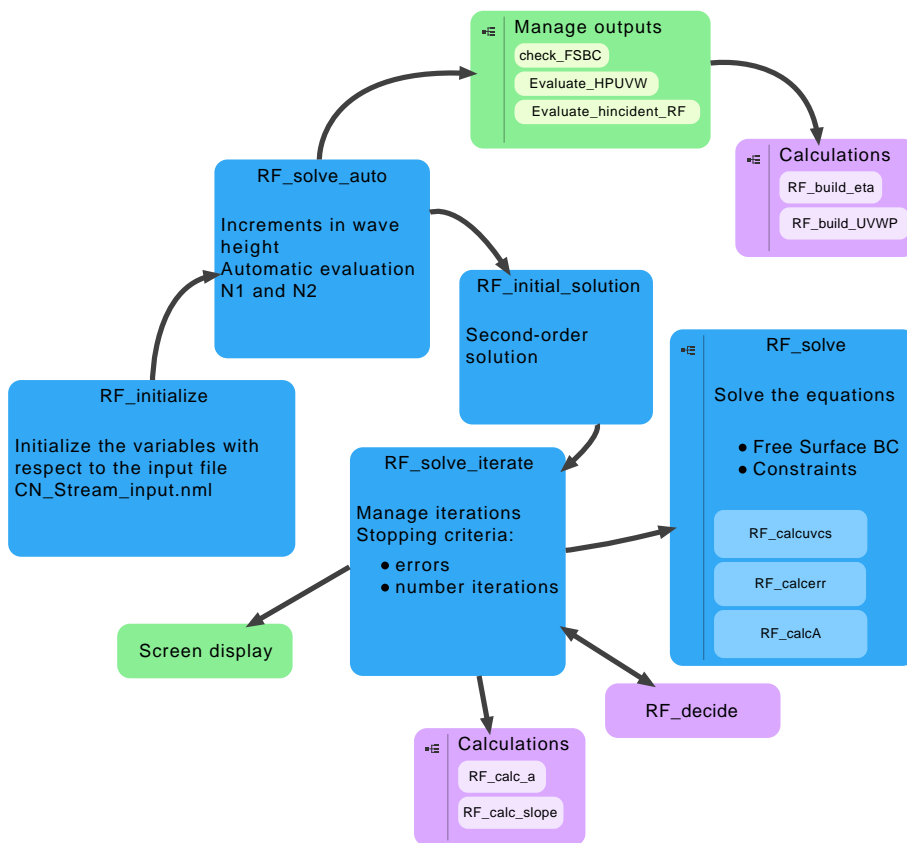


Figure 18: Schematic view of CN-Stream algorithm.

RF_solve_auto manages the automatic calculations of the numerical parameters at use in CN-Stream. This contains the specific enhancements proposed in the code as detailed in Sec. 1.5.

RF_solve_iterate manages the iterations in the solution procedure and the corresponding stopping criteria relative to the errors/tolerances (minimum amplitude of the modes, inversion of the system, etc.) as well as the maximum number of iterations.

RF_solve is the effective solution of the linear system of equations described previously: it is the core of the original stream function procedure.

Note that for internal communications and library use in other Fortran programs, CN-Stream uses Fortran types to reduce the number of passing arguments. An example is also provided to link the library with C++ program (in particular OpenFOAM), in this case the library is interrogated to provide flow quantities at a certain position and time.

3.1. Source files

3.1.1. Project organisation and dependency

The main folder consists in:

- `CMakeLists.txt`
- `example` Folder with examples of using the library through the communication module from Fortran and C++
- `src` Folder with source files (include also the sources of libFyMc)
- `input` Folder with input file example
- `output` Default folder output

The code use the library libFyMc to read the “dictionary” input file. The library is provided with the sources.

3.1.2. CN-Stream - variables and types

The different Fortran types (`RF_type`, `option_type`, `output_type`) are defined explictely in `variables_CN_Stream.h` and `variables_output_CN_Stream.h` and are included when needed in CN-Stream. It allows the user to include them easily into CN-Stream but also in another code, which makes use of the CN-Stream library.

In more details, those types include:

- `RF_type`
 - definition of the parameters of the wave, corresponding to the input parameters specified in the input file as detailed in Sec. 3.3.1
 - Modal amplitudes of the free surface elevation η and of the velocity potential ϕ (or equivalently the stream function ψ).
 - If needed, free surface elevation and slope in the spatial domain.
- `option_type`: all options relative to the solution method, specified in input file as detailed in Sec. 3.3.1. This type also includes the optimal number of points N_1 and N_2 resulting from the procedure detailed in Sec. 1.5.2.
- `output_type`: defines for one location (X, Y, Z) the free surface elevation, the pressure and velocity components together with the necessary time and/or spatial derivatives of those components. The possible existence of a Y -component is associated to the definition of an angle of propagation as input, referenced as θ .

3.1.3. CN-Stream - main program

The set of Fortran files needed in order to compile CN-Stream is listed in Tab. 7 with a brief description of the purpose of each of the source file.

CN-Stream source files	
mod_CN_Stream.f90	Module allowing communication without using complex datatypes (C++)
main_CN_Stream.f90	Main program for CN-Stream computations
modSolve.f90	Solves the equation of the problem described above
modCNinitialize.f90	Initialization of CN-Stream computation
modUtils.f90	Useful functions
modMatrix.f90	Computes the inverse matrix from the least square method
modType.f90	Definition of types and useful constants
modModal.f90	Useful functions used in modSolve.f90
HOS_modlinear_wave.f90	Computation of linear dispersion relation
HOS_modmaths.f90	Useful mathematical functions
modSetupNameList.f90	Read the input NML file
modReconstrucVol.f90	Evaluate wave elevation, pressure, velocity and its derivatives
modReconstruction.f90	Recompute wave elevation, pressure, velocity and wave slope from Fourier coefficients and the other way around .
modOutputs.f90	Write outputs on files.
variables_CN_Stream.h	Definition of Fortran types: RF_type and option_type
variables_output_CN_Stream.h	Definition of Fortran type: output_type

Table 7: List of source files used in CN-Stream

3.1.4. CN-Stream - library

For the possible use of CN-Stream as a library in another program, the set of Fortran files is similar to the one described in previous subsection. There are two ways to use CN-Stream as a library.

- Use the declarations of the variables of the `variables_CN_Stream.h` and `variables_output_CN_Stream.h` and call the functions described in the source file `lib_CN_Stream.f90`.
- Use the subroutines indicated in the communication module `mod_CN_Stream.f90`.

3.2. Compilation

The code can be compiled on any computer architecture. One only needs a Fortran compiler (for instance gfortran, the GNU Fortran compiler, part of GCC). A makefile is provided but the recommended procedure is to use cmake. The following commands can be executed in the root folder where `CMakeLists.txt` is located, to compile the dependency, the executable and the shared library:

- `cmake -H. -Bbuild`
- `cmake --build build`

Compilation has been tested with gfortran on different Unix/Linux platforms as well as in Windows environment.

For Windows environment, compilation using Intel Visual Studio has also been tested. The program is provided with the corresponding project file `CN_Stream.vfproj` allowing a straightforward compilation of the code.

3.3. Running CN-Stream

CN-Stream has been developed for command-line run with an input file located in the `input` folder containing all specifications needed. All output files will be created in the directory `output`, but other specifications can be given. Details of inputs and outputs are provided hereafter. The executable can be run with the command `./mainCNS`. The name of the dictionary can be specified as an argument.

3.3.1. Inputs

CN-Stream needs as input the characteristics of the wave, together with some informations relative to the numerical solution of the problem (target accuracy, etc.). The wave can be described in dimensional or non-dimensional form. As a matter of clarity, the wave parameters to provide as input are detailed in the next paragraphs depending on the need of the user. Note that those parameters are provided within an input file which content is also detailed.

In CN-Stream, the non-linear regular water wave is characterized by:

- the water depth h , possibly infinite,
- the wave length λ or the wave period T ,
- the wave height H (distance from crest to trough),
- the constant current superimposed to the wave (under the form of a Eulerian current or a given transport of mass).

Input file. The input file is assumed to be named `CN_Stream_input.dict`. Table 8 describes the different parameters accessible in this input file. The `Options_solver` parameters are useful for an advanced user, in order to obtain solutions with a controlled accuracy and/or to look for waves close to the wave breaking limit.

3.3.2. Output files

Depending on the choices made in the input file (see Tab.8), different output files are created. They are located at the root of the folder. Input file also defines if outputs are dimensional or non-dimensional quantities. Following files may be created:

- `waverf.cof` gives the main important parameters of the simulation, namely λ , H , k , T , c , c_S , c_E , $N_1 + 1$, $N_2 + 1$, R , h (in dimensional or non-dimensional form depending on the value of input: `GeneralDimension` in the input file) as well as the modal amplitudes a_n and b_n ,
- `waverf.dat` gives the modal amplitudes a_n and b_n .

In complement, different subroutines may be called to write the necessary outputs needed by the user. They are available inside the source files and a simple call in the main program will enable the corresponding outputs:

- `WriteOutput`: this subroutine creates the file `resultsOutput.txt` containing at a given location and time all spatial quantities computed by CN-Stream (free surface elevation, velocities, pressures, derivaitves, etc.).
- `TecplotOutput_Modes`: this subroutine creates the file `Modes_CN_Stream.dat` containing the modal description of the free surface elevation and velocity potential, for use with Tecplot.
- `TecplotOutput_VelocityPressure`: this subroutine creates the file `VP_card_fitted.dat` containing the velocity and pressure field under the simulated wave, for use with Tecplot.
- `TecplotOutput_FreeSurface`: this subroutine creates the file `FreeSurface_CN_Stream.dat`, which provides the free surface elevation and slope.

waveInput: Label (waveStream in example file) and Definition of the characteristics of the simulated wave	
GeneralDimension	Dimensional (=1) or Non-dimensional (=0)
GeneralDepth	h if GeneralDimension=1 / h' if GeneralDimension=0
GeneralModes	Number of modes for first evaluation
WaveInput	Period / Wavelength (if GeneralDimension=0 only Wavelength is possible)
Period	period value if WaveInput set to Period
Wavelength	Wavelength value if WaveInput set accordingly
WaveHeight	H if GeneralDimension=1 / H' if GeneralDimension=0
CurrentValue	value of current ; dimensional if input: GeneralDimension=1 / non-dimensional if input: GeneralDimension=0
CurrentType	type of current ; 1 mass transport / 0 eulerian current
Options for the numerical solution of the problem	
n_H	n_H : Number of steps in wave height
err_type	Error type: 0 absolute ; 1 relative
eps_err	$\epsilon_F^{rel/abs}$ Tolerance on the equations
err_max	$\max(\epsilon_F)$: Error value over which computation is considered divergent
eps_inc	$\epsilon_Z^{rel/abs}$: Convergence criteria on the unknowns
eps_N1	ϵ_{N1} : Decision criteria on the modes for the automatic adjustment of N_1
itermax	Maximum number of iterations
increment_type	choose between a linear or exponential incrementation: Increment type for wave height / 0 linear ; 1 exponential
printonscreen	print the intermediate results of the simulation on the command prompt: Print on screen =1 / do not print on screen = 0
writeoutput	Write output files =1 / do not Write output files = 0
subdict	Standard way to include dictionary (here "Output" in another using libFyMc)
Outputs: supplementary info for outputs	
Path	Specify output path (default: "./output/")
x/y/z/time	Specify position to evaluate quantities for local outputs (default:"0.0")
theta	Incident angle of waves (default:"0.0")

Table 8: Description of input file parameters for CN-Stream

4. Conclusions

CN-Stream has been developed to compute non-linear regular ocean waves with a high level of accuracy. The model is limited to arbitrary constant water depth and non-breaking waves. CN-Stream is an open-source code, redistributed under the terms of the GNU GPL v3 License as published by the Free Software Foundation. It is available through the GitHub platform [9]. Along with the source code, a Wiki documentation is available, which makes the compilation of the source files and the execution easy. It can be used as a stand-alone binary or as a library to be included in another program.

The code is based on the stream function theory and the original works of [26] and [15] have been taken as basis. Some enhancements are proposed in the current implementation, namely: i) a possible different number of modes to represent the free surface elevation and the stream function (or eq. the velocity potential) and ii) an automatic calculation of the optimal number of collocation points (or equivalently of the number of modes) to reach a target accuracy.

It has been demonstrated that these allow an increase accuracy of the numerical solution, together with an extended domain of application with respect to the maximum wave height accessible.

Different example of applications of the model are provided, which demonstrate the importance of the non-linear effects in the description of a regular waves. The free surface profiles are analyzed over a wide range of steepness and relative water depth, together with the kinematics and pressure fields.

The volume fields are a standard output of CN-Stream, which intends to provide a simple and accurate code for the description of non-linear regular waves, especially in the context of wave-structure interactions. It is worth noticing that it is already at use in different codes dealing with wave-structure interactions at Centrale Nantes. Among other, CFD codes such as ICARE [24, 25], WCCH [21] or OpenFoam [20] uses CN-Stream as a library for the description of incident non-linear regular waves.

References

References

- [1] F. Bonnefoy, G. Ducrozet, D. Le Touzé, and P. Ferrant. *Advances in Numerical Simulation of Nonlinear Water Waves*, volume 11 of *Advances in Coastal and Ocean Engineering*, chapter Time domain simulation of non linear water waves using spectral methods. World Scientific, 2010.
- [2] John R Chaplin. Developments of stream-function wave theory. *Coastal Engineering*, 3:179–205, 1980.
- [3] JE Chappellear. Direct numerical calculation of wave properties. *Journal of Geophysical Research*, 66(2):501–508, 1961.
- [4] YoungMyung Choi, Maite Gouin, Guillaume Ducrozet, Benjamin Bouscasse, and Pierre Ferrant. Grid2grid: HOS wrapper program for cfd solvers. *arXiv preprint arXiv:1801.00026*, 2017.
- [5] Didier Clamond. Remarks on bernoulli constants, gauge conditions and phase velocities in the context of water waves. *Applied Mathematics Letters*, 74:114–120, 2017.
- [6] Didier Clamond and Denys Dutykh. Accurate fast computation of steady two-dimensional surface gravity waves in arbitrary depth. *Journal of Fluid Mechanics*, 844:491–518, 2018.
- [7] ED Cokelet. Steep gravity waves in water of arbitrary uniform depth. *Philosophical Transactions of the Royal Society of London A: Mathematical, Physical and Engineering Sciences*, 286(1335):183–230, 1977.
- [8] RG Dean. Stream function representation of nonlinear ocean waves. *Journal of Geophysical Research*, 70(18):4561–4572, 1965.
- [9] LHEEA Res. Dept. Open-source release of CN-Stream. <https://github.com/LHEEA/CN-Stream/wiki>.
- [10] G. Ducrozet, H. B. Bingham, A. P. Engsig-Karup, F. Bonnefoy, and P. Ferrant. A comparative study of two fast nonlinear free-surface water wave models. *Int. J. Numer. Meth. Fl.*, 69(11):1818–1834, 2012. doi: 10.1002/fl.2672.
- [11] Guillaume Ducrozet, Félicien Bonnefoy, David Le Touzé, and Pierre Ferrant. A modified high-order spectral method for wavemaker modeling in a numerical wave tank. *European Journal of Mechanics-B/Fluids*, 34:19–34, 2012.
- [12] Guillaume Ducrozet, Félicien Bonnefoy, David Le Touzé, and Pierre Ferrant. Hos-ocean: Open-source solver for nonlinear waves in open ocean based on high-order spectral method. *Computer Physics Communications*, 203(Supplement C):245–254, 2016.
- [13] A.P. Engsig-Karup, H.B. Bingham, and O. Lindberg. An efficient flexible-order model for 3d nonlinear water waves. *Journal of Computational Physics*, 228(6):2100–2118, 2009.
- [14] J. D. Fenton. The numerical solution of the steady water wave problem. *Comp. & Geosc.*, 14(3):357–368, 1988.
- [15] JD Fenton. The numerical solution of steady water wave problems. *Computers & Geosciences*, 14(3):357–368, 1988.
- [16] JD Fenton. Nonlinear wave theories. *the Sea*, 9(1):3–25, 1990.

- [17] JK Hunter and J-M Vanden-Broeck. Solitary and periodic gravity-capillary waves of finite amplitude. *Journal of Fluid Mechanics*, 134:205–219, 1983.
- [18] Niels G Jacobsen, David R Fuhrman, and Jørgen Fredsøe. A wave generation toolbox for the open-source CFD library: OpenFOAM®. *International Journal for Numerical Methods in Fluids*, 70(9):1073–1088, 2012.
- [19] Bernard Le Méhauté. *An Introduction to Hydrodynamics and Water Waves*. Springer, 1976.
- [20] Z. Li, B. Bouscasse, G. Ducrozet, L. Gentaz, and P. Ferrant. Progress in coupling potential flow theory and navier-stokes equations for wave-structure interaction problems. In *Proceedings of the 37nd International conference on Ocean, Offshore and Artic Engineering (OMAE), Madrid, Spain*, 2018.
- [21] Z. Li, G. Oger, and D. Le Touzé. A VOF-based finite volume scheme for numerical simulation of weakly-compressible two-phase flows using high-order WENO reconstruction. *Journal of Computational Physics (submitted)*, 2017.
- [22] A. Miche. *Mouvements ondulatoire de la mer en profondeur croissante ou décroissante. forme limite de la houle lors de son déferlement. application aux digues maritimes. troisième partie. forme et propriétés des houles limites lors du déferlement. croissance des vitesses vers la rive*. Annales des Ponts et Chaussées, 1944.
- [23] G. Oger, D. Le Touzé, G. Ducrozet, J. Candelier, and P.-M. Guilcher. A Coupled SPH-Spectral Method for the Simulation of Wave Train Impacts on a FPSO. (45400):V002T08A088, 2014.
- [24] G. Reliquet, A. Drouet, P.-E. Guillerm, E. Jacquin, L. Gentaz, and P. Ferrant. Simulation of wave-body interaction using a single phase Level Set function in the SWENSE method. In *Proceedings of the 32nd International conference on Ocean, Offshore and Artic Engineering (OMAE), Nantes, France*, 2013.
- [25] R. Reliquet, Y. Zhang, Z. Li, Y. Choi, Z. Li, B. Bouscasse, L. Gentaz, and D. Le Touzé. Assessment of different cfd methods capability to accurately simulate wave propagation. In *Proceedings of the 37nd International conference on Ocean, Offshore and Artic Engineering (OMAE), Madrid, Spain*, 2018.
- [26] M. M. Rienecker and J. D. Fenton. A Fourier approximation method for steady water waves. *J. Fluid Mech.*, 104:119–137, 1981.
- [27] Leonard W Schwartz. Computer extension and analytic continuation of stokes’ expansion for gravity waves. *Journal of Fluid Mechanics*, 62(3):553–578, 1974.
- [28] Rodney J Sobey, Peter Goodwin, Robert J Thieke, and Robert J Westberg Jr. Application of stokes, cnoidal, and fourier wave theories. *Journal of waterway, port, coastal, and ocean engineering*, 113(6):565–587, 1987.
- [29] G.G. Stokes. On the theory of oscillatory waves. *Trans. Cambridge Philos. Soc.*, 8:441–455, 1849. Math. Phys. Pap. 1 : 197-229.
- [30] J-M Vanden-Broeck and LW Schwartz. Numerical computation of steep gravity waves in shallow water. *The Physics of Fluids*, 22(10):1868–1871, 1979.
- [31] JM Williams. Limiting gravity waves in water of finite depth. *Philosophical Transactions of the Royal Society of London A: Mathematical, Physical and Engineering Sciences*, 302(1466):139–188, 1981.
- [32] Xiaoxu Zhong and Shijun Liao. On the limiting stokes wave of extreme height in arbitrary water depth. *Journal of Fluid Mechanics*, 843:653–679, 2018.